

Semileptonic four-fermion final states in polarised reactions: Exact results vs an improved narrow width approximation

M. Baillargeon¹, G. Belanger² and F. Boudjema²

1. Grupo Teorico de Altas Energias, Instituto Superior Tecnico
Edifcio Ciências (Física) P-1096 Lisboa Codex, Portugal

2. Laboratoire de Physique Theorique ENSLAPP
Chemin de Bellevue, B.P. 110, F-74941 Annecy-le-Vieux, Cedex, France.

Abstract

We calculate the process $e^+e^- \rightarrow \mu^+\mu^- \gamma$ with the full set of Feynman diagrams. We consider different implementations of the W width and different combinations of the photon polarisations. The results of an improved narrow width approximation based on $e^+e^- \rightarrow W^+W^-$ with full spin-correlations that takes into account different angular cuts as well as cuts on the invariant masses are compared to those of the complete calculation.

1 Introduction

During the past few years there has been an intense activity in the physics potentials of a linear e^+e^- collider which, in a first stage, could be operating at centre-of-mass energies around the $t\bar{t}$ threshold to 500 GeV with a later upgrade to 1.5-2 TeV [1]. The clean environment of the machine will definitely settle the issue of a light Higgs and allow for precision measurements to be conducted. Most prominent among these, especially if no Higgs has been discovered, is a detailed investigation of the dynamics of the weak bosons since they are a window on the mechanism of symmetry breaking through their Goldstone/longitudinal component [2].

Another attraction of the linear collider is that it can be turned into a $\gamma\gamma$ collider through Compton scattering of a laser beam on the single pass electrons [3]. The resulting collider will thus have a centre-of-mass energy corresponding to about as much as 80% of the total e^+e^- energy. One can also arrange to have an almost monochromatic spectrum while maintaining a good luminosity. Moreover, the photons are easily polarised. In this type of colliders one of the most important processes is $\gamma\gamma \rightarrow W^+W^-$ with a cross section reaching very quickly, after threshold, a plateau of about 80 pb. With a contemplated luminosity of about 20 fb^{-1} at 500 GeV this would mean some millions of W pairs. This statistics will thus allow a very precise measurement of the photonic couplings of the W , a subject that has been widely studied [4-9].

The reaction $\gamma\gamma \rightarrow W^+W^-$ has been studied by various authors and the one-loop radiative corrections have already been calculated [10]. For a more thorough investigation of this most important reaction at the photon collider, it is essential to evaluate the 4-fermion final states in $\gamma\gamma$ processes. The full evaluation of these final states is important because they are not only reached by $\gamma\gamma \rightarrow W^+W^-$ but also through contributions that do not proceed via the doubly resonant W channel. The latter could be considered as a potentially important background to $\gamma\gamma \rightarrow W^+W^-$ and therefore stand in the way of a precise investigation of $\gamma\gamma \rightarrow W^+W^-$. The same need for the evaluation of all 4-fermion final states was required for LEP 2. Consequently a large number of groups undertook the task of providing as a precise as possible calculation of the 4-fermion cross-sections in e^+e^- [11,12]. The aim of this paper is to do the same for $\gamma\gamma$ initiated 4-fermion processes specialising first in semi-leptonic final states $l\bar{l}q\bar{q}$ for energies currently being discussed for the next linear collider. Prior to this paper there appeared only one evaluation of $\gamma\gamma \rightarrow l\bar{l}q\bar{q}$ processes by Moretti [13]. Moreover, the latter has not addressed the important issue of the photon polarisations and no attempt has been made to compare the results of the full 4-fermion calculations including all possible diagrams with some

approximation based on the $W W$ resonant diagrams. We will therefore give a special attention to the photon polarisation and will show that once moderate cuts are applied, a calculation based on $\gamma \rightarrow W^+ W^-$ and which takes into account the full spin correlations can reproduce, at the per-cent level or even better, the result of the complete set of diagrams after allowing for a smearing factor. We will also consider different schemes for the implementation of the W width and whenever appropriate we will compare our results with those of Moretti [13].

2 On-Shell W pair production and decay with full spin correlations and smearing

2.1 Tree-level helicity amplitudes for $\gamma \rightarrow W^+ W^-$ in the SM

To understand the characteristics of the $W^+ W^-$ cross-section it is best to give all the helicity amplitudes which contain a maximum of information on the reaction.

It is important to specify our conventions. We work in the centre of mass of the incoming photons and refrain from making explicit the azimuthal dependence of the initial state. The total energy of the system is \sqrt{s} . We take the photon with helicity λ_1 (λ_2) to be in the $+z$ ($-z$) direction and the outgoing W^- (W^+) with helicity λ_- (λ_+) and 4-momentum p_- (p_+):

$$p_- = \frac{\sqrt{s}}{2} (1; \sin \theta; 0; \cos \theta); \quad q = \frac{\sqrt{s}}{2} (1; -\sin \theta; 0; -\cos \theta); \quad s = M_W^2; \quad (2.1)$$

The polarisations for the helicity basis are defined as

$$\begin{aligned} \epsilon_{\lambda_1}(\lambda_1) &= \frac{1}{\sqrt{2}} (0; \lambda_1; i; 0) & \epsilon_{\lambda_2}(\lambda_2) &= \frac{1}{\sqrt{2}} (0; \lambda_2; i; 0) & \epsilon_{\lambda_-}(\lambda_-) &= \\ \epsilon_{\lambda_+}(\lambda_+) &= \frac{1}{\sqrt{2}} (0; \cos \theta; i; \sin \theta) & \epsilon_{\lambda_-}(\lambda_-) &= \frac{1}{\sqrt{2}} (0; \cos \theta; i; \sin \theta) & \epsilon_{\lambda_+}(\lambda_+) &= \\ \epsilon_{\lambda_-}(\lambda_-) &= \frac{1}{\sqrt{2}} (\sin \theta; 0; \cos \theta) & \epsilon_{\lambda_+}(\lambda_+) &= \frac{1}{\sqrt{2}} (\sin \theta; 0; \cos \theta) & \epsilon_{\lambda_-}(\lambda_-) &= 0: \end{aligned} \quad (2.2)$$

^yTotal cross sections for purely QED 4-fermion production through $\gamma \gamma \rightarrow W^+ W^-$ have been considered for quite sometime [14]. Leptonic final states of the kind $\gamma \gamma \rightarrow e^+ e^-$ have first been evaluated by Couture [15]. The (unpolarised) results for the other leptonic channels have very recently been presented in [16].

We obtain for the tree-level SM helicity amplitudes^z:

$$M_{1/2; +} = \frac{4}{1 - \cos^2 \theta} N_{1/2; +}; \quad (2.3)$$

where

$$\begin{aligned} N_{1/2; 00} &= \frac{1}{8} [4(1 + \cos \theta) + (1 - \cos \theta)(4 + \cos^2 \theta) \sin^2 \theta]; \\ N_{1/2; 0} &= \frac{s}{8} (1 - \cos \theta)(1 + \cos \theta) \sin \theta; \\ N_{1/2; +} &= \frac{s}{8} (1 - \cos \theta)(1 + \cos \theta) \sin \theta; \\ N_{1/2; -} &= (1 + \cos \theta)(1 + \cos \theta) + \frac{1}{2} [8(1 + \cos \theta) + (1 + \cos \theta)(3 + \cos \theta) \\ &\quad + 2(1 - \cos \theta)(1 + \cos \theta) \cos^2 \theta + 4(1 - \cos \theta)(1 + \cos \theta) \cos^2 \theta \\ &\quad + (1 - \cos \theta)(1 + \cos \theta) \cos^2 \theta] \sin^2 \theta = : \end{aligned} \quad (2.4)$$

With the conventions for the polarisation vectors, the fermionic tensors that describe the decay of the W 's are defined as in [17]. In particular one expresses everything with respect to the W where the arguments of the D -functions refer to the angles of the particle (i.e. the electron, not the anti-neutrino), in the rest-frame of the W , taking as a reference axis the direction of flight of the W (see [17]). The D -functions to use are therefore $D_{\lambda; 0}^W(\theta; \phi) = D_{\lambda; 0}$, satisfying $D_{\lambda; 0} = D_{0; \lambda}$ and:

$$\begin{aligned} D_{+; } &= \frac{1}{2} (1 - \cos^2 \theta) e^{2i\phi}; & D_{-; 0} &= \frac{1}{2} (1 - \cos \theta) \sin \theta e^{i\phi}; \\ D_{-; } &= \frac{1}{2} (1 - \cos \theta)^2; & D_{0; 0} &= \sin^2 \theta : \end{aligned} \quad (2.6)$$

The angle θ_e is directly related to the energy of the electron (measured in the laboratory frame):

$$\cos \theta_e = \frac{1}{\beta} \frac{4E_e}{\sqrt{s}} - 1 : \quad (2.7)$$

There are a few remarks one can make about the structure of the W^+W^- helicity amplitudes. First of all, because of the t-channel spin-1 exchange, the W 's are produced predominantly in the forward/backward direction. An effect that is more pronounced as the energy increases. The production of longitudinal W 's occurs predominantly when the

^zThese formulae had already been derived by us [4,5] albeit with a different convention for the polarisation vectors. They are also consistent with those given by Yehudai [6] and more recently by Choi and Hagiwara [9] after allowing for the different conventions for the polarisation vectors.

photons are in a $J_z = 2$ configuration. Otherwise the amplitudes for longitudinal W 's are at least a factor $M_W = \sqrt{s}$ smaller than the amplitudes for transverse W 's. Another very interesting property is that for like-sign photon helicities only like-sign W helicities are produced. Moreover, as the energy increases this occurs with the photons transferring their helicities to the W 's. Therefore for like-sign photon helicities, the cross section is dominated by $++; ++$ and $--; --$.

2.2 Five-fold differential cross section

The five-fold differential cross section can now be easily obtained. In the narrow width approximation and for definite photon helicities as defined above the five-fold differential cross section $d\sigma_5 / (d\cos\theta_1 d\cos\theta_2 d\cos\theta_3 d\cos\theta_4 ds)$ writes

$$\begin{aligned} & \frac{d\sigma_5}{d\cos\theta_1 d\cos\theta_2 d\cos\theta_3 d\cos\theta_4 ds} = B_W^{f_1 f_2} B_W^{f_3 f_4} \frac{3}{32} \frac{1}{s} \frac{1}{8} \\ & \times \sum_{\lambda_1, \lambda_2, \lambda_3, \lambda_4} M_{1; 2; \lambda_1 \lambda_2}^+(s; \cos\theta_1) M_{1; 2; \lambda_3 \lambda_4}^0(s; \cos\theta_2) D_{\lambda_1 \lambda_2}^0(\theta_3; \cos\theta_1) D_{\lambda_3 \lambda_4}^0(\theta_4; \cos\theta_2) \\ & \times \frac{d\sigma}{d\cos\theta} = \frac{3}{8} B_W^{f_1 f_2} B_W^{f_3 f_4} \\ & \times \sum_{\lambda_1, \lambda_2, \lambda_3, \lambda_4} D_{\lambda_1 \lambda_2}^0(\theta_3; \cos\theta_1) D_{\lambda_3 \lambda_4}^0(\theta_4; \cos\theta_2) \\ & \text{with } \sum_{\lambda_1, \lambda_2, \lambda_3, \lambda_4} D_{\lambda_1 \lambda_2}^0(\theta_3; \cos\theta_1) D_{\lambda_3 \lambda_4}^0(\theta_4; \cos\theta_2) = \frac{M_{1; 2; \lambda_1 \lambda_2}^+(s; \cos\theta_1) M_{1; 2; \lambda_3 \lambda_4}^0(s; \cos\theta_2)}{\sum_{\lambda_1, \lambda_2, \lambda_3, \lambda_4} |M_{1; 2; \lambda_1 \lambda_2}^+(s; \cos\theta_1)|^2 |M_{1; 2; \lambda_3 \lambda_4}^0(s; \cos\theta_2)|^2}; \quad (2.8) \end{aligned}$$

where θ is the scattering angle of the W and ρ is the density matrix. Note that one separates the decay and the production parts. To be able to reconstruct the direction of the charged W and to have least ambiguity in reconstructing the $W W$ process, the best channel is the semi-leptonic channel $W \rightarrow l \bar{\nu}_l; W \rightarrow jj^0$ with $l = e, \mu$.

This very compact formula makes it possible to impose cuts on the escape angles and energies of the fermions. However, because of the nature of this narrow width approximation which is actually a zero-width approximation, the invariant mass of each fermion pair is equal to the W -mass.

To improve the above approximation and to make it possible to take into account cuts on the invariant mass of the decay products of the W one can introduce a smearing over the invariant masses, s_\pm , of the W . Customarily one has [18,19], as with the $e^+ e^- \rightarrow W^+ W^-$ cross section, convoluted over the doubly on-shell $W^+ W^-$ cross section:

$$\sigma_W \sim \int_0^{Z_s} ds_W \sigma_W(s_W) \int_0^{Z_{\sqrt{s}} - \sqrt{s_W}} ds_+ \sigma_W(s_+) \delta(W^+ W^-)(s_+; s_-); \quad (2.9)$$

with

$$\sigma_W(x) = \frac{1}{(x - M_W^2)^2 + M_W^2} : \quad (2.10)$$

This prescription is not gauge invariant. $\sigma_{W+W}(s_+; s_-)$ is derived from an on-shell amplitude which is not an element of the S-matrix. Although $\sigma_{W+W}(s_+; s_-)$ refers pictorially to doubly "resonant" diagrams, it contains pieces that are only singly resonant, beside other parts that are not resonant at all. To wit, one can expand $\sigma_{W+W}(s_+; s_-)$ as

$$\begin{aligned} \sigma_{W+W}(s_+; s_-) = & \sigma_{W+W}(s_+ = M_W^2; s_- = M_W^2) \\ & + (s_- - M_W^2) S(s_+) + (s_+ - M_W^2) S(s_-) + N(s_+; s_-) : \end{aligned} \quad (2.11)$$

The first part, $\sigma_{W+W}(s_+ = M_W^2; s_- = M_W^2)$ is the genuine on-shell W^+W^- cross section which is gauge invariant and that we have used to derive the density matrix. However the functions S and N are not gauge invariant and must be combined with the complete set of the 4-fermion diagrams. A problem that we will address in the next section. Therefore to improve on the approximation for the density matrix, we will simply convolute the on-shell fully correlated cross section Eq. 2.8 $\sigma_{W+W}(s_+ = M_W^2; s_- = M_W^2)$ $\sigma_{W+W}(s)$, to obtain

$$\begin{aligned} \sigma_W &= R \sigma_{W+W}(s) \\ &= \sigma_{W+W} \int_{f_1 f_2 f_3 f_4} (s) \int_0^{\sqrt{s}} ds \sigma_W(s) \int_0^{(\sqrt{s} - \sqrt{s_{\text{cut}}})^2} F_{\text{cut}}(s_+; s_-) ds_+ \sigma_W(s_+); \end{aligned} \quad (2.12)$$

where we have introduced a function F_{cut} which takes into account the cuts that we may impose on the invariant masses, s_{\pm} . R is the reduction factor introduced by the width and the invariant mass cuts. The above formula can also be applied when other cuts on the decay products are imposed, as long as these cuts do not implicitly or explicitly involve s_{\pm} . In this case the factorisation holds with $\sigma_{W+W}(s)$ calculated through the fully correlated amplitudes.

For invariant mass cuts such that,

$$\sqrt{s} \geq M_W \quad ; \quad (2.13)$$

one has

$$\begin{aligned} R = & \frac{1}{2} \left(A \tan^{-1} \frac{(2M_W + \sqrt{s})}{M_W} + A \tan^{-1} \frac{(2M_W - \sqrt{s})}{M_W} \right)^2 \\ & - A \tan^{-1} \frac{2}{M_W} \left((2M_W)^2 \right) : \end{aligned} \quad (2.14)$$

If the invariant mass cuts on s are different, $\sqrt{s} \approx M_W$, the reduction factor is the product of the square root of the above formulae with $\sqrt{s} \approx M_W$ for one of the factors and $\sqrt{s} \approx M_W$ in the second. However if one imposes an invariant mass cut on only one of the W , a very good approximation for the reduction factor is

$$R \approx \frac{1}{2} \left(A \tan^{-1} \frac{(2M_W + \sqrt{s})}{M_W} + A \tan^{-1} \frac{(2M_W - \sqrt{s})}{M_W} \right) \left(A \tan^{-1} \frac{M_W}{\sqrt{s}} + A \tan^{-1} \frac{(\sqrt{s} - 2M_W)}{M_W} \right) \quad (2.15)$$

In the case where no cut on the invariant masses is imposed, to take the width effect into account one can apply the approximate formula

$$R \approx 1 - \frac{1}{2} \frac{M_W^2}{s} + \frac{M_W^2}{s} \frac{M_W^2}{M_W^2} + \frac{M_W^2}{s} \frac{M_W^2}{2M_W^2} \frac{1}{s} : \quad (2.16)$$

3 Complete calculation of four-fermion production

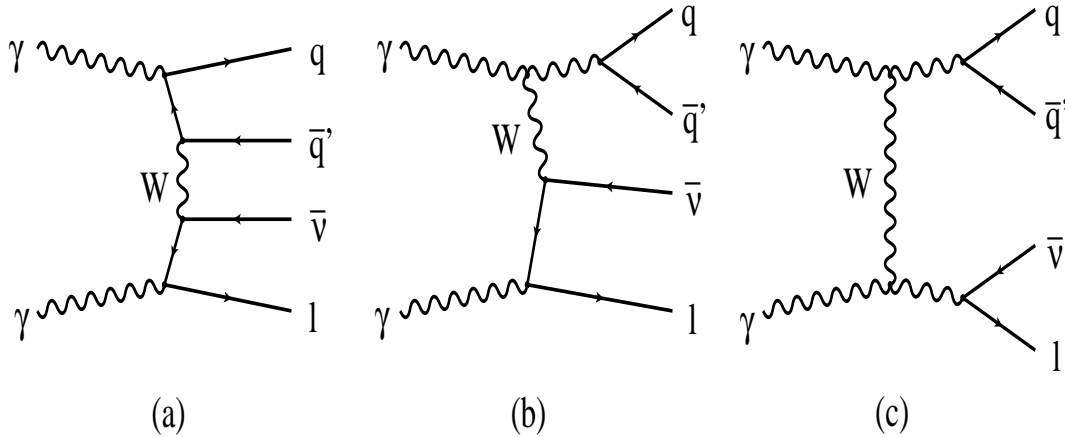


Figure 1: Classes of Feynman diagrams that contribute to the semi-leptonic four-fermion production in e^+e^- . In the narrow width approximation only diagrams of type (c) is considered. Type (b) may be associated to single W^+ production while type (a) are non-resonating.

The tree-level calculation of $e^+e^- \rightarrow q\bar{q}l\bar{l}$ involves the evaluation of 21 diagrams in the unitary gauge (see Fig.1), while the narrow width approximation is based on a mere 3 diagrams. As we have seen, the narrow width approximation can be improved by taking

into account finite width effects even when cuts on the invariant mass of the decay products of the W 's are envisaged. Since this approximation leads to very compact analytical formulae it is important to quantify how good this approximation can be compared to the full calculation of the 4-fermion final state.

Beside those going through WW , some of the latter 4-fermion final states may be associated to single W production of the sort $\gamma \rightarrow e^- e^+ W^+$ with the subsequent decay of the W^+ (see Fig.1, diagram (b)). This type of contribution is important for very forward electrons with a typical escape angle for the electron of order $m_e = \sqrt{s}$. For these very forward events it should be possible to revert to an approximation based on a structure function approach (density of electrons in the photon). We will not be concerned with these types of events since our motivation is to fully reconstruct the WW events which requires the observation of the charged fermion as well as the jets in the central region. This is especially important if one wants to investigate New Physics effects affecting the W sector through $\gamma \rightarrow W^+ W^-$. These require one to be able to fit angular distributions of the fermions through, for example, a maximum likelihood method [20].

As for events with very forward jets, another complication arises if very forward jet-tagging is not possible. In this situation one needs to consider other contributions beyond the 21 diagrams leading to $\gamma \rightarrow e^- e^+ u d$. These additional contributions are due to the non-perturbative hadron component of the photon and thus need a special treatment. We therefore concentrate on the $l_1 l_2$ (and its conjugate) signature with observable charged particles. We have therefore imposed a cut on the charged fermions such that:

$$|\cos \theta_{l_1 j}| < 0.98 \quad \cos \theta_{l_2 j} < 0.9 \quad (3.17)$$

Moreover we also imposed a cut on the energies of the charged fermions:

$$E_f > 0.125 \sqrt{s} \quad (3.18)$$

We take $\alpha = (0) = 1/137$ for the WW vertex as we are dealing with an on-shell photon. The result of the full one-loop corrections to $\gamma \rightarrow W^+ W^-$ [10] indicates also that this is the effective coupling constant for $\gamma \rightarrow W^+ W^-$. We also take $M_W = 80.22$ GeV and the width of the W , is $\Gamma_W = \Gamma_W(M_W^2) = 2.08$ GeV. The partial width of the W into jets and $l_1 l_2$ is calculated by taking at the W vertex the effective couplings $(M_W^2) = 1/128$ and $\sin^2 \theta_W = 0.23$.

In order to quantify the effect of the "non doubly resonant" contributions and how well the approximation based on the density matrix approach fares, we have considered

different cuts on the invariant mass (see 2.13) of the jets (p_{jj}) and the leptonic pair (p_{ll}). Especially because for a realistic set-up where the photon energy is not known in an event by event basis, we have also relaxed the cut on the leptonic invariant mass. Two values on the invariant mass of the pairs were considered. A stringent cut $p_{ll} = 5 \text{ GeV}$ and a cut that is more realistic when dealing with a jet pair: $p_{jj} = 18 \text{ GeV}$.

There is another issue that needs to be discussed before we present our results. This concerns the implementation of the width in the W propagators. This important issue has received quite a lot of attention recently in connection with 4-fermion production in e^+e^- [19,21,22]. The introduction of the width is necessary if one is to integrate over all virtualities of the W 's. The naive way of providing the W propagators either with a running or fixed width does not lead to a gauge-invariant 4-fermion matrix element, since only one subset (the one corresponding to the "resonant" diagrams) of the whole 4-fermion diagrams has received a "correction". Prior to the introduction of the width, the complete 4-fermion amplitude is gauge invariant, while the resonant diagrams are gauge invariant by themselves only when the W are both on mass-shell as calculated in the previous section. To remedy this situation, introduced by "correcting" the two-point function, it has been suggested to implement radiative corrections to the three-point as well as to the four-point vertices [21,23]. This is quite cumbersome to implement on the 4-fermion final state and at the Monte-Carlo level, moreover these additional corrections need to be carried at all orders in perturbation theory while up to now this approach has been implemented only at the one-loop level. Different other schemes or rather simplified tricks have been suggested and implemented in most of the $e^+e^- \rightarrow 4f$ existing programs (for a review see [19,21,22]), but on a formal level none is satisfactory. On a practical level, it is found [19], for $e^+e^- \rightarrow W^+W^-$, that after implementing cuts (in our case tagging the jets and the electron/positron) all schemes agree quite well. To quantify the sensitivity to the W width implementation we have implemented a fixed width, a running width as well as what is called a "fudge-factor" [24]. The fudge factor amounts to first generating all the 4-fermion helicity amplitudes with zero width, that is the W propagators have the simple form $1/(k^2 - M_W^2)$ and thus gauge invariance is guaranteed. One then applies an overall fudge-factor $(k^2 - M_W^2)/(k^2 - M_W^2 + i \Gamma_W M_W)^x$ to the whole amplitude. Since we consider energies where the doubly-resonant diagrams give a large contribution this fudge factor should be a good approximation. Related to this issue we have also investigated the effect of picking up among the 21 4-fermion diagrams, those three that correspond to the double W exchange, where the W may be on-shell. The amplitudes

*One may also apply a running width here.

thus generated lead to the "on-shell cross sections" defined in Eq. 2.9. As we argued above, unless we restrict s to be very close to M_W^2 , we expect gross deviations from the result of the evaluation of the full set of diagrams. This will be clearly substantiated in our results.

The helicity amplitudes based on the full set of contributions were reproduced through the automatic program Madgraph [25] and checked with GRACE [26]. The numerical phase space integration was done with the help of VEGAS [27]. As a first comparison, we have tuned our set of input parameters and cuts to those chosen by Moretti [13] and have reproduced his results for the unpolarised cross sections.

3.1 Results and Comparison

Our results including the different implementations and approximations are presented in Tables 1 – 3. Before commenting on the comparisons, let us stress that for any approximation or implementation of the width, even after different cuts are imposed the two $J_z = 2$ configurations must be equal, i.e., one must have $\sigma_{++} = \sigma_{--}$ which is a direct consequence of the fact that the cuts we used are the same in the "forward" and "backward" directions and that the initial particles are identical (Bose symmetry). This is well rendered by our calculations as evidenced from the Tables. The very slight differences (below the permil) that the tables show for these combinations of photon helicities are a measure of the precision of our MC (Monte-Carlo) integration. We have preferred to keep both the σ_{++} and σ_{--} entries in our tables so that their relative precision be used as a benchmark for a comparison between the different approximations. We have considered three typical centre-of-mass energies: 400, 800 and 1600 GeV corresponding to e^+e^- centre-of-mass energies of 500, 1000 and 2000 GeV.

On the other hand one should not expect to have $\sigma_{++} = \sigma_{--}$ when cuts are introduced. Indeed, consider the case of the narrow width approximation with full spin correlations. For like-sign photon helicities we remarked that only same-helicity W 's were produced. Moreover, the overwhelming contributions were those with transverse W 's whereby each photon transfers its helicity to the W . Before cuts are introduced $\sigma_{++} = \sigma_{--}$. However, because of the chiral structure of the W couplings, the electron is emitted in a preferential direction depending on the helicity of the W . Indeed, taking the W flight direction as a reference axis, in its rest frame a left-handed W emits an electron in the forward direction (see 2.6) while for a right-handed W the electron is backward. At the energies we are considering both W 's are very forward/backward (in the laboratory system) moreover the

$\sqrt{s} = 400 \text{ GeV}$						
$1 \ 2$	Inv. M ass. Cuts	Narrow W idth Im proved	A ll diag. $W (M_W^2)$	A ll diag. $W (s)$	A ll diag. Fudge	\Resonant" Subset
$++$	None	2288	2310	2312	2309	2354
$+$	None	1893	1926	1927	1923	1975
$+$	None	1890	1927	1927	1926	1975
$++$	None	2186	2184	2183	2183	2252
$++$	$jj; 1 < 5 \text{ GeV}$	1759	1762	1764	1761	1761
$+$	$jj; 1 < 5 \text{ GeV}$	1455	1458	1458	1456	1456
$+$	$jj; 1 < 5 \text{ GeV}$	1454	1457	1458	1457	1456
$++$	$jj; 1 < 5 \text{ GeV}$	1681	1683	1681	1682	1682
$++$	$jj; 1 < 18 \text{ GeV}$	2158	2167	2169	2165	2166
$+$	$jj; 1 < 18 \text{ GeV}$	1785	1793	1794	1791	1793
$+$	$jj; 1 < 18 \text{ GeV}$	1783	1795	1794	1794	1793
$++$	$jj; 1 < 18 \text{ GeV}$	2061	2063	2061	2061	2068
$++$	$jj < 5 \text{ GeV}$	2006	2026	2027	2024	2035
$+$	$jj < 5 \text{ GeV}$	1660	1682	1682	1679	1695
$+$	$jj < 5 \text{ GeV}$	1658	1683	1683	1683	1696
$++$	$jj < 5 \text{ GeV}$	1917	1921	1920	1921	1948
$++$	$jj < 18 \text{ GeV}$	2222	2245	2247	2243	2257
$+$	$jj < 18 \text{ GeV}$	1838	1865	1866	1863	1881
$+$	$jj < 18 \text{ GeV}$	1836	1866	1866	1865	1881
$++$	$jj < 18 \text{ GeV}$	2123	2127	2125	2125	2159

Table 1: Comparison between the different approximations for the calculation of $e^+e^- \rightarrow \gamma\gamma \rightarrow W^+W^-$ for a centre-of-mass energy of 400 GeV. $1,2$ refer to the helicities of the two photons. Cuts other than those on the invariant mass are given in the text. "Narrow width Improved" refers to the approximation based on the density matrix and takes into account smearing. The next column is the result based on the complete set of the 4-fermion diagrams with a fixed width. "All diag." $W (s)$ is with a running width, while "Fudge" implements a fudge factor as explained in the text. The last column gives the result of keeping only the $W W$ 4-fermion diagrams, i.e. based on the on-shell W^+W^- amplitudes (where a fixed width is used). All cross sections are in fb.

$\sqrt{s} = 800 \text{ GeV}$						
1 2	Inv. Mass. Cuts	Narrow Width Improved	All diag. (M_W^2)	All diag. (s)	All diag. Fudge	\Resonant" Subset
+ + + + + + + + +	None	1274	1290	1290	1287	1399
	None	1010	1034	1032	1032	1119
	None	1009	1037	1035	1036	1121
	None	1232	1260	1259	1259	1335
+ + + + + + + + +	$jj; 1 < 5 \text{ GeV}$	979	983	982	982	983
	$jj; 1 < 5 \text{ GeV}$	777	776	775	776	776
	$jj; 1 < 5 \text{ GeV}$	776	777	777	777	778
	$jj; 1 < 5 \text{ GeV}$	947	950	947	948	950
+ + + + + + + + +	$jj; 1 < 18 \text{ GeV}$	1201	1207	1205	1203	1211
	$jj; 1 < 18 \text{ GeV}$	952	953	951	952	956
	$jj; 1 < 18 \text{ GeV}$	951	954	954	954	958
	$jj; 1 < 18 \text{ GeV}$	1162	1164	1162	1163	1167
+ + + + + + + + +	$jj < 5 \text{ GeV}$	1117	1128	1127	1126	1164
	$jj < 5 \text{ GeV}$	886	899	898	899	926
	$jj < 5 \text{ GeV}$	885	902	901	901	928
	$jj < 5 \text{ GeV}$	1080	1097	1095	1096	1123
+ + + + + + + + +	$jj < 18 \text{ GeV}$	1237	1250	1249	1246	1294
	$jj < 18 \text{ GeV}$	981	996	994	995	1029
	$jj < 18 \text{ GeV}$	980	999	998	998	1031
	$jj < 18 \text{ GeV}$	1197	1214	1213	1213	1247

Table 2: As in Table 1 but for $\sqrt{s} = 800 \text{ GeV}$.

$\sqrt{s} = 1600 \text{ GeV}$						
$1 \ 2$	Inv. Mass. Cuts	Narrow Width Improved	All diag. M_W^2	All diag. s	All diag. Fudge	\Resonant" Subset
$++$	None	377	389	389	389	456
$+$	None	320	335	335	335	388
$+$	None	320	336	336	336	391
$++$	None	427	447	447	447	490
$++$	$jj; 1 < 5 \text{ GeV}$	290	291	291	291	291
$+$	$jj; 1 < 5 \text{ GeV}$	246	246	246	246	246
$+$	$jj; 1 < 5 \text{ GeV}$	246	246	247	246	247
$++$	$jj; 1 < 5 \text{ GeV}$	328	329	329	330	329
$++$	$jj; 1 < 18 \text{ GeV}$	356	357	357	357	358
$+$	$jj; 1 < 18 \text{ GeV}$	302	302	302	302	302
$+$	$jj; 1 < 18 \text{ GeV}$	302	303	303	303	304
$++$	$jj; 1 < 18 \text{ GeV}$	403	404	404	405	405
$++$	$jj < 5 \text{ GeV}$	331	337	336	337	355
$+$	$jj < 5 \text{ GeV}$	281	288	288	289	302
$+$	$jj < 5 \text{ GeV}$	281	289	289	289	303
$++$	$jj < 5 \text{ GeV}$	375	385	385	385	398
$++$	$jj < 18 \text{ GeV}$	366	373	373	373	393
$+$	$jj < 18 \text{ GeV}$	311	319	319	320	336
$+$	$jj < 18 \text{ GeV}$	311	320	320	320	336
$++$	$jj < 18 \text{ GeV}$	415	426	426	427	442

Table 3: As in Table 1 but for $\sqrt{s} = 1600 \text{ GeV}$

boost for the electron is substantial. This has the effect that for a left-handed W^- the electron is emitted very forward in the lab system, but when an electron from a right-handed W^- is boosted it tends to be further away from the beam than is the electron from a left-handed electron W^- . As a result, this means that if one only cuts on forward-backward electrons (with respect to the beam) the cross section with left-handed photons will be smaller than that with right-handed photons $++$. This has been explicitly checked by our calculations. In the tables one clearly sees that the argument we have given above leading to $++ >$ is explicitly confirmed both at 400 and 800 GeV, but seems to fail for $\sqrt{s} = 1600$ GeV. The reason the above argument does not lead to $++ >$ at this very high energy has to do with the fact that the other cuts we have taken, more specially cuts on the energy of the electron and on the angles of the quarks/antiquarks, become very restrictive at this energy with an effect that counterbalances and washes out that of the simple description in terms of the angular cut on the electron. For instance, take the cut on the energy of the electron, $E_e > 0.125 \sqrt{s}$, which is directly related to the angle θ_e that defines the direction of the electron in the rest frame of the W^- (see Eq. 2.6-2.7). All events pass this cut at 400 GeV and practically all pass this cut at 800 GeV, but not at 1600 GeV. However, events that are rejected by this cut, effectively on θ_e , correspond to electrons that are backward (in the rest frame of the W^-) therefore it is the electrons that originate from a right-handed W^- that will be penalised. These were the ones that, after boosting, passed the cuts of forward/backward electrons (with respect to the photon beam), i.e. our previous argument becomes ineffective at 1600 GeV. In fact, it turns out that the angular cut on the jets is even more penalising. First, if only this cut is imposed and since it is symmetric for the quark and the antiquark then $++ =$ for all energies. However, at very high energies the boost of the fermions becomes so large that the angular cut on the jets that we have applied is tantamount to having imposed the same angular cut on the W^+ , i.e. θ , and therefore on the W^- angle. Consequently, the cut on the angle of the electron with the beam becomes redundant and does not cut many of the electrons from a left-handed W^- . This has also been checked explicitly by our calculations.

From the tables one sees that, for all energies, for all combinations of photon helicities and independently of the invariant mass cuts, the results are not very sensitive to how the width has been implemented on the all four-fermion final state. The discrepancies if any, are below the permil level and thus consistent with our MC error. A similar

[†] Fig. 2 and Fig. 3 show the drastic difference between the distributions in the energy of the electron produced in the $++$ and $++$ configurations. These distributions may be easily understood by the argument based on the $\cos \theta_e$.

conclusion was reached in the case of $e^+e^- \rightarrow W^+W^-$ so long as extreme forward electrons were rejected (this almost eliminates the t-channel photon exchange) [19]. For the rest of the discussion, we will therefore compare the results of the improved narrow width approximation, those of keeping the "on-shell W cross section Eq. 2.9) with what one obtains with the full set of diagrams. As we discussed earlier, this "on-shell" subset is expected to violate gauge invariance. We find that when no cuts on the invariant masses are imposed the results one obtains with this subset are not to be trusted for any configuration of the photon helicities, especially as the energy increases. At 400 GeV the discrepancy with the exact result is about 3% and increases to 17% (!) at 1600 GeV for $++$. It is only by imposing cuts on both leptonic and hadronic invariant masses that the "on-shell" subset (even for 1600 GeV) reproduces the complete calculation and this even when the invariant mass cut is 18 GeV. However, as soon as one relaxes the cut on one of the invariant masses, namely the W , even a strict cut on the jet system of 5 GeV is not enough to make the results in accord with those of the complete calculation. As expected the discrepancy grows with the centre-of-mass energy and as the invariant mass cut gets loose. This is also a manifestation of how a loss of gauge invariance can translate into a loss of unitarity.

The narrow width approximation with full spin correlation taking into account the smearing factor fares much better than the "on-shell" (Eq. 2.9) and turns out to be a good approximation. With a 5 GeV cut on both the leptons and the jets the narrow width approximation reproduces the results of the complete calculation within the MC errors for all combinations of helicities and for all energies. When the cut is relaxed to 18 GeV, the discrepancy is never larger than 3 permil and is within the errors for certain combinations of the photon helicities. If a cut of 18 GeV on the hadronic system only is imposed the agreement worsens, and for the lower energies it affects the different configurations of the photon helicities differently. For instance, with our set of cuts, at 400 GeV is reproduced at the permil level by the improved narrow width approximation while $++$ and the $J_z = 2$ are off by one per-cent. On the other hand, at 800 GeV while the agreement remains sensibly the same for $++$ and very slightly worsens in the $J_z = 2$ to be off 1.3%, for $+-$ one has agreement at off 1.5%. At 1600 GeV the agreement for $++$ is below 2% while for the other photon helicities it reaches 3%. At this particular energy, one may thus have to revert to the result based on the complete set of diagrams. If one would like to keep more statistics by not imposing an invariant mass cut neither on the hadronic nor the leptonic system, the narrow width approximation generally does not describe the results of the 4-fermion final state, especially as the energy increases. It is only with the particular helicity $+-$ at 400 GeV that the agreement is within the

per mil, otherwise the discrepancy at 400 and 800 GeV is about 1–2% reaching 4–5% at 1600 GeV. Nonetheless, these results are clearly far better than the ones obtained with the on-shell WW cross section ("resonant" subset).

Another important issue to check is whether our improved narrow width approximation reproduces the various distributions. For instance one may wonder whether the excellent agreement for the σ_{tot} at 400 GeV at the level of the integrated cross section is fortuitous. That is, does the approximation reproduce the various distributions one obtains with the full set of diagrams as well as it reproduces the integrated cross section? or could the distributions be different and yet agree when integrated over all the events? To analyse this issue, we have looked at two distributions, the energy of the electron and the angle of the electron with the beam. Note that for the latter, non resonant diagrams whereby a photon splits into an electron/positron pair can contribute substantially when the electron is very forward. Therefore this distribution could indicate if the cut on the forward electrons that we have imposed could be made stricter in order to reach a better agreement with the "exact" result.

To illustrate our point we restrict ourselves to the case σ_{tot} at 400 GeV and $\sigma_{e^+e^-}$ at 800 GeV, and only study the realistic case where a cut of 18 GeV is imposed on the jets only. At 400 GeV one sees that both the angular and the energy distributions are reproduced extremely well (see Fig. 2). In fact comparing the distributions, side by side, one can hardly see the discrepancies. To better quantify the agreement we looked at the relative difference between the two distributions. For the energy distribution the agreement is always below the per-cent (the peaks one observes in the bins at the lower and upper ends have very low statistics and are not to be trusted). For the angular distribution, the agreement fluctuates between 1–2% and 2% in some of the bins, but for $\cos\theta_e > 0.8$ where the distributions peak and where the events are concentrated the agreement is much better. One can make the same statement about the distributions at 800 GeV (see Fig. 3). The distributions are reproduced quite well and the agreement is of the same order as the one reached for the integrated cross section, a slightly less good agreement is observed only in regions that are much less populated. For instance, the relative difference in the angular distribution of the electron is maximum for events in the central region.

One can therefore conclude by saying that as long as moderate cuts on the di-jet invariant mass are imposed, the narrow width approximation including full spin correlations and smearing reproduces the results of the complete 1_{jj} channel at the per-cent level for energies up to 1 TeV, and even much better at energies around 400 GeV. Above the TeV,

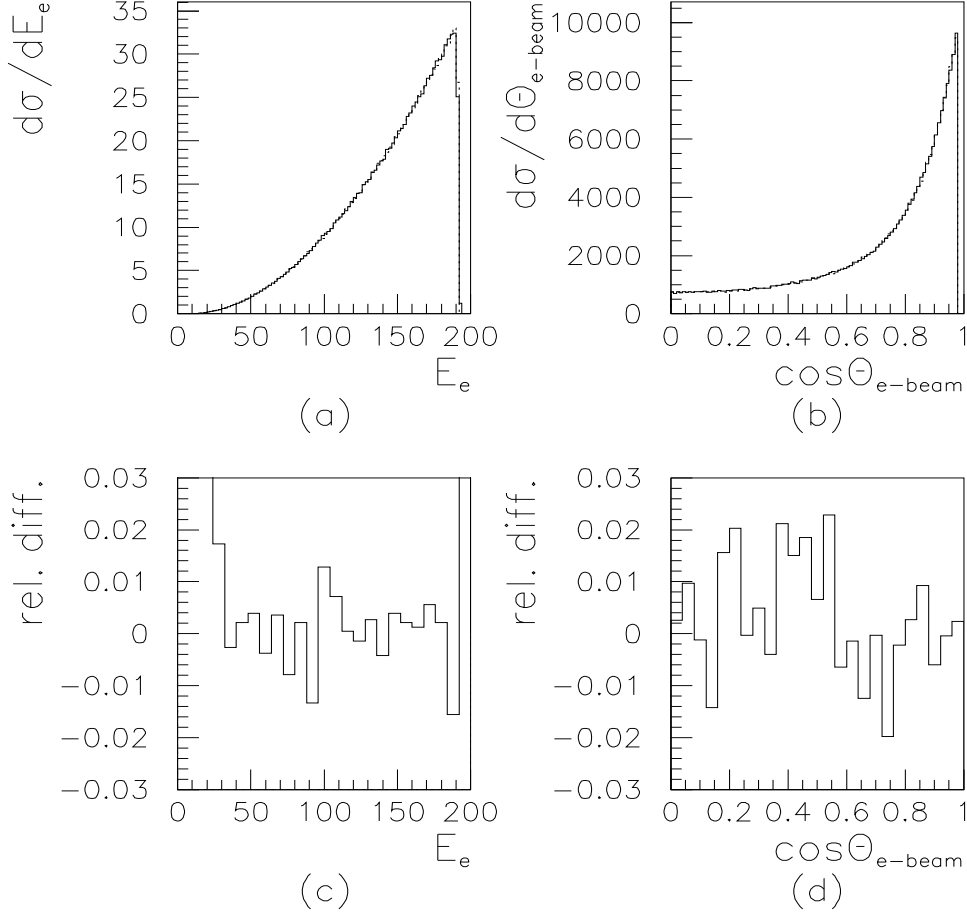


Figure 2: Comparison between the distributions obtained with the improved narrow width approximation and with the computation based on the complete set of diagrams for a centre-of-mass energy of 400 GeV with both photons being left-handed ($\gamma_L\gamma_L$). A cut of 18 GeV on the invariant mass of the jets has been imposed. All other cuts are as specified in the text. Shown are the distribution in the energy of the electron, E_e (a), and the cosine of the angle of the electron with the beam $\cos\Theta_{e\text{-beam}}$ (b) where the dotted line are for the approximation. The differences are hardly noticeable on these distributions. In order to better show the discrepancies, we plot in Figs. (c) and (d) the relative difference between the two distributions $(\text{Exact} - \text{Approx})/\text{Exact}$.

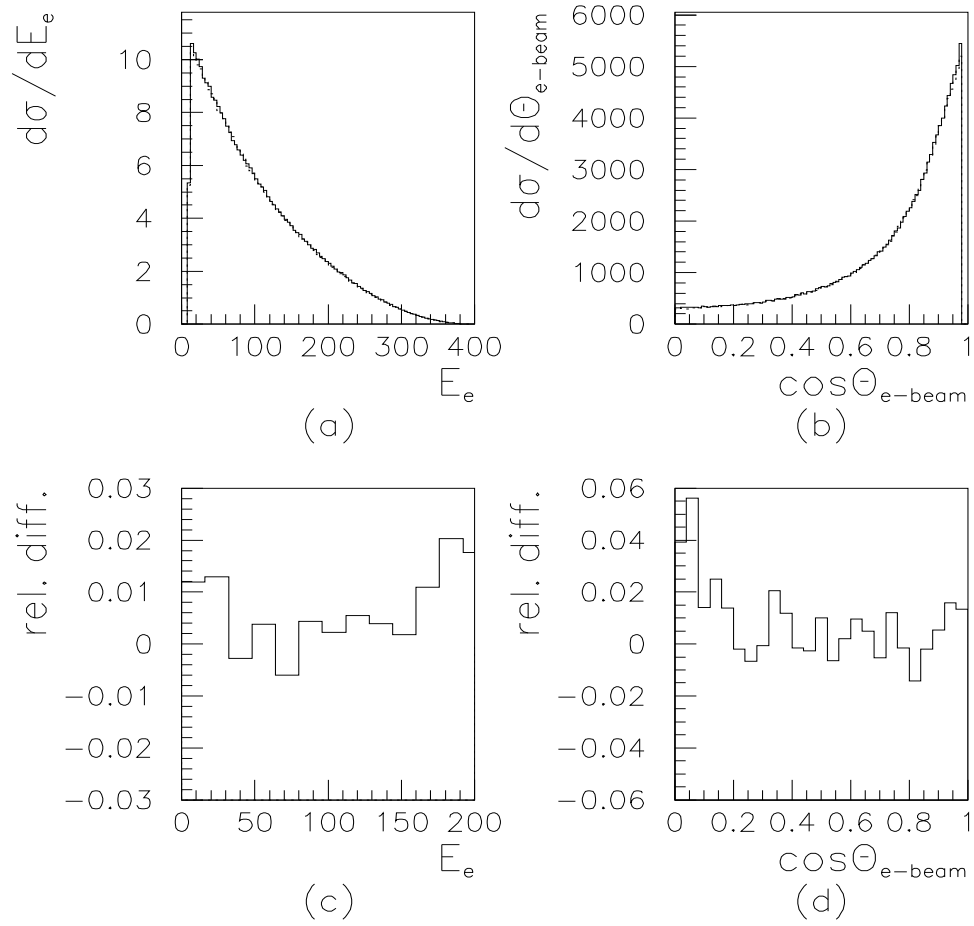


Figure 3: As with the previous figure but for a centre-of-mass energy of 800 GeV and with both photons being right-handed $++$.

unless much stricter invariant mass cuts are imposed (meaning a loss of statistics), for precision measurements one needs to rely on the result of the complete calculation based on the full set of diagrams describing the 4-fermion final states. The latter computation, with the requirement that one keeps particles within the central region, is not sensitive to the different implementations of the W width. We also find that when the agreement at the level of the integrated cross section is obtained the distributions are reproduced with the same accuracy especially in regions where one has the bulk of the events.

To simulate a more realistic set-up one should have convoluted our cross sections with polarised luminosity functions that describe the energy spectrum of the photons. This could be very easily implemented especially with the improved narrow width approximation. Most of the analyses on the laser induced physics have taken an ideal spectrum based on a theoretical calculation of this spectrum [3] that does not simulate the full conditions of the conversion of an electron beam by an intense laser. More realistic simulations of the spectrum have only very recently been considered [28]. Because of the uncertainty in these spectra we have preferred not to consider any particular spectrum especially that our principal aim was to provide a calculation for four-fermion final states in polarised reactions and to enquire whether an approximation based on the resonant $W W$ diagrams would be sufficient for future analyses.

References

[1] For reviews see:

Proc. of the Workshop on e^+e^- Collisions at 500 GeV: The Physics Potential, ed. P. Zerwas, DESY-92-123A,B (1992).

ibid DESY-93-123C (1993) and DESY-96-123D (1996).

Proceedings of the LCW 95, Physics and Experiments with Linear Colliders, Morioka, Japan, Sep. 1995, Edts Miyamoto et al., World Scientific, 1996.

H. Murayama and M. Peskin, hep-ex/9606003.

[2] For a recent review on W physics at the linear colliders see, F. Boudjema, Proceedings of the Workshop on Physics and Experiments with Linear e^+e^- Colliders, LCW 95, Edts. Miyamoto et al., p. 199, Vol. I, World Scientific, 1996.

[3] I.F. Ginzburg, G.L. Kotkin, V.G. Serbo and V.I. Telnov, Sov. ZhETF Pis'ma 34 (1981) 514 [JETP Lett. 34 491 (1982)];

I.F. Ginzburg, G.L. Kotkin, V.G. Serbo and V.I. Telnov, Nucl. Instrum. Methods 205 (1983) 47;

- I.F. Ginzburg, G.L. Kotkin, S.L. Pan'filov, V.G. Serbo and V.I. Telnov, *ibid* 219 (1984) 5;
 V.I. Telnov, *ibid* A 294 (1990) 72;
 V.I. Telnov, *Proc. of the Workshop on "Physics and Experiments with Linear Colliders"*, Saariselka, Finland, eds. R. Orawa, P. Eerola and M. Nordberg, World Scientific, Singapore (1992) 739;
 V.I. Telnov, in *Proceedings of the IXth International Workshop on Photon-Photon Collisions.*, edited by D.O. Caldwell and H.P. Paar, World Scientific, (1992) 369.
- [4] M. Baillargeon, G. Belanger and F. Boudjema, in *Proceedings of Two-photon Physics from DA NE to LEP 200 and Beyond*, Paris, eds. F. Kapusta and J. Parisi, World Scientific, 1995 p. 267; hep-ph/9405359.
- [5] G. Belanger and F. Boudjema, *Phys. Lett. B* 288 (1992) 210.
- [6] E. Yehudai, *Phys. Rev. D* 44 (1991) 3434.
 E. Yehudai, Ph.D. thesis, August 1991, SLAC-383.
- [7] S.Y. Choi and F. Schrempp, *Phys. Lett. B* 272 (1991) 149.
- [8] G. Belanger and G. Couture, *Phys. Rev. D* 49 (1994) 5720.
- [9] S.Y. Choi, K. Hagiwara and M.S. Baek, *Phys. Rev. D* 54 (1996) 6703.
- [10] A. Denner and S. Dittmaier and R. Schuster, *Nucl. Phys. B* 452 (1995) 80.
 G. Jikia, in *Physics with e^+e^- Colliders*, the European Working Groups, DESY-96-123D, Op. cit and Freiburg preprint Dec. 96, Freiburg-THP 96/23, hep-ph/9612380.
- [11] See the *Standard Model Processes* report, conv. F. Boudjema and B. Mele, in the LEP 2 Yellow Book, CERN 96-01, p. 207, Vol. 1, ed. by G. Altarelli, T. Sjöstrand and F. Zwirner.
- [12] See the *Event Generators for W W* report, conv. D. Bardin and R. Kleiss, in the LEP 2 Yellow Book, p. 3, Vol. 2, Op. cit.
- [13] M. Moretti, hep-ph/9604303, Apr. 1996.
- [14] H. Cheng and T.T. Wu, *Phys. Rev. D* 1 (1970) 3414;
 L.N. Lipatov and G.V. Frolov, *Sov. J. Nucl. Phys.* 13 (1971) 333.
- [15] G. Couture, *Phys. Rev. D* 44 (1991) 2755.

- [16] M .M oretti, hep-ph/9606225, Jun. 1996.
- [17] M .B ilenky, J.L .K neur, F M .Renard and D .Schildknecht, Nucl.Phys.409 (1993) 22.
- [18] T .M uta, R N ajiñ a and S.W akaizum i, M od. Phys. Lett. A 1 (1986) 121.
- [19] For an up-to-date review , see the W W cross sections and distributions report, conv. W .Beenakker and F .A .Berends, in the LEP 2 Yellow Book, p. 79, Vol. 1, Op. cit .
- [20] M .Baillargeon, G .Belanger and F .Boudjē m a, ENSLAPP preprint, ENSLAPP-A-636/97, Jan. 97 .
P relim inary results have been discussed in: M .Baillargeon et al, hep-ph/9603220, in P roceedings of Physics with Linear Colliders, the European W orking G rups, DESY -96-123D , Op. cit .
- [21] E N .A rgyres et al, Phys.Lett. B 358 (1995) 339.
- [22] Beenakker et al, N IK H EF P reprint, N IK H EF -96-031, D ec. 96. hep-ph/9612260.
- [23] U .Baur and D .Zeppenfeld, Phys.Rev.Lett.75 (1995) 1002.
- [24] D .Zeppenfeld, J .A .M .Vern aseren and U .Baur, Nucl.Phys.B 375 (1992) 3.
- [25] T .Stelzer and W .F .Long, Autom atic generation of tree-level helicity amplitudes, M AD -PH -813, Jan. 1994, hep-ph/9401258.
- [26] T .Ishikawa, T K aneko, K K ato, S K awabata, Y Shin izu and K Tanaka, KEK Report 92-19, 1993, The GRACE m anual Ver. 1.0.
- [27] See G P .Lepage, J .Com p. Phys. 27 (1978) 192.
- [28] For an update see V .V .Telhov, in Photon '95, edited by D .J .M iller, S.L .Cartw right and V .K hoze, W orld Scienti c, Singapore 1995.
See also, D .J .Schulte, in P roc. of the W orkshop on e^+e^- Collisions at 500 GeV : The Physics P otential, ed. P .Zerwas, DESY -96-123D (1996).